Discovery of a multipotent cell type from the term human placenta

Sangeetha Vadakke-Madathil[1*], Bingyan J Wang[1], Micayla Oniskey[1], Fumiko Dekio[2], Rachel Brody[2], Shari Gelber[3], Rhoda Sperling[4] and Hina W. Chaudhry[1*]

[1]Department of Cardiology, [2]Department of Pathology, [3]Department of Obstetrics/Gynecology and Maternal-Fetal Medicine, Icahn School of Medicine at Mount Sinai, New York, NY, USA

Abstract

The human placenta is a reservoir of a multitude of cell types with immense regenerative potential. Caudal-type homeobox-2 (CDX2) is a conserved factor that regulates trophectoderm formation and placentation during early embryonic development and hence can play a vital role in understanding developmentally conserved regenerative mechanisms. Cdx2 lineage tracing in our previous study identified multipotent Cdx2 lineage cells in the mouse placenta capable of restoring cardiac function after intravenous delivery in male mice with experimental cardiac injury (myocardial infarction). Here we demonstrate that CDX2-expressing cells are prevalent in the human chorionic placenta and are uniquely committed to cardiovascular differentiation. We examined the term placentas from 106 healthy donors and showed that isolated CDX2 cells can spontaneously differentiate into cardiomyocytes, functional vascular cells, and retain homing ability *in vitro*. Functional annotation from transcriptomics analysis supports enhanced cardiogenesis, vasculogenesis, immune modulation, and chemotaxis gene signatures in CDX2 cells. CDX2 cells can be clonally propagated in culture with retention of cardiovascular differentiation. Bringing us a step closer to translation, our study identifies an easily accessible and ethically feasible cell source to facilitate therapeutic strategies for cardiovascular disease.

Main

The successful use of cell therapy for cardiac repair hinges on several critical attributes: cells must have the capacity for cardiomyocyte differentiation akin to embryonic stem cells (ES) and induced pluripotent cells (iPSC), they must have clonality, possess an immune-modulatory capacity for allogeneic administration, and ideally the ability to home to sites of injury. Cell therapy for cardiac purposes has been demonstrated to be safe by numerous preclinical and clinical studies[1-4], however; the lack of *bona fide* cardiac differentiation amongst cell types administered in clinical trials thus far remains a challenge[5-7]. Despite targeted cell therapy approaches, the heart is still the most challenging organ to repair due to its limited regenerative potential and lack of meaningful contribution of existing cell sources towards *de novo* cardiomyocyte formation. Regenerative biology hinges on exploring evolutionarily preserved healing mechanisms to maintain and restore homeostasis. Gestation is one such condition that requires extensive cellular cross-talk to maintain homeostasis. The human placenta is a vital organ responsible for supporting embryonic development and facilitating the exchange of nutrients and waste between the mother and fetus. Placenta and the fetal heart are thought to undergo concurrent evolution sharing major developmental pathways[8-10]. Studies suggest that the placenta may regulate cardiac ventricular wall expansion once maternal blood flow is established[11]. This implies that cells with regenerative ability within the placenta may be better poised to support cardiogenesis. Stem or progenitor cells from the placenta are easily obtainable and are developmentally closer to embryonic stem cells but functionally different and non-tumorigenic[12]. Caudal type homeobox-2 (CDX2) is a conserved factor expressed by trophoblast stem cells that regulate trophoblast stem cell differentiation and is required for proper placental development[13,14]. We have discovered a novel role of Cdx2 cells in murine gestation as a preclinical model of myocardial infarction (MI) in pregnant mice elicited the

specific migration of fetal placental cells into the injured maternal heart to form cardiovascular cells[15]. Furthermore, isolated murine placental Cdx2 lineage cells formed spontaneously beating cardiovascular cells *in vitro* and contributed to cardiac repair *in vivo* after intravenous infusion even in male mice subjected to myocardial infarction[16].

Healthy human term placentas can be an abundant source of cells with regenerative potential. In this study, we isolated CDX2-expressing cells using a human CDX2 promoter-driven lentivirus-based mCherry fluorescence reporter from 106 human term placentas. Transcriptomic analyses comparing human embryonic cells, term placental CDX2 cells, and term placental non-CDX2 cells were performed to gain deeper insights into the functional differences between these cell types. We further investigate the stem/progenitor function and cardiovascular commitment of human placental CDX2 cells to ascertain their potential as a novel therapeutic for cardiovascular disease.

Results

Cells expressing CDX2 are enriched within the chorionic region of the human placenta

The homeodomain protein CDX2 is involved in embryonic development and placentation. To detect if CDX2 is present in human placentas, we carried out a multi-parametric approach and examined the transcript expression from an earlier time point in first-trimester chorionic villus samples (CVS) and later within the chorionic cells (fetal) from term healthy placentas. CDX2 mRNA was detected in both CVS and chorionic regions (**Fig.1a**). Sanger sequencing and analysis of the output FASTA sequences further confirmed sequences specific to human CDX2 mRNA (Supplemental data). Immunoblot analyses detected CDX2 protein in the term chorion (~40kDa) with the conventional doublet pattern representing two isoforms from alternative splicing (**Fig. 1b**). HeLa cells showed a lower endogenous expression of CDX2, whereas DLD1 served as a

positive control. Immunohistochemistry revealed that CDX2 protein was enriched in the fetal chorionic region of the human placenta and not in the fetal amnion (Extended Data **Fig.1a,b**). CDX2 was detected in the villous region (**Fig 1c**), particularly within the cytotrophoblast layer of the chorion (Extended Data Fig.1a,b). We found that most CDX2-expressing cells co-localized with the trophoblast marker Cytokeratin 7 (**Fig. 1c, d**, CKT7- 95 ± 5.0%) and were associated with Human Leukocyte Antigen G (**Fig. 1e, f,** HLAG- 50.5±5%), which is mostly expressed in extravillous trophoblast progenitors and is critical for inducing an immune-tolerant microenvironment in the placenta. This data shows that CDX2 is expressed in the term human placenta and expresses pan trophoblast marker cytokeratin 7 and extravillous marker HLA-G.

Clonality, *in vitro* expansion, and homing potential of CDX2 cells

The initial isolation of viable cells expressing CDX2 was challenging because no surface markers had been identified for enrichment thus far. In this study, we developed a CDX2 promoter-driven lentivirus-based approach to select cells expressing CDX2 (Extended Data Fig.2a-c and methods). Based on the transduction efficiency and mCherry fluorescence, out of three candidates, a sequence containing 612bps of CDX2 promoter (promoter 1) was selected (Extended Data Fig.2d-g, also see supplemental data) and within the multiplicities of infection (MOI) ranging from 20-100 MOI (Extended Data Fig.2h-q), the 50MOI range was further chosen.

Following initial culturing, chorionic cells from term placentas were transduced with the chosen lentivirus to select CDX2mCherry positive cells (**Fig. 2a**). Flow cytometry-based sorting of transduced chorionic cells from various placentas revealed that the frequency of CDX2mCherry cells ranged from 1.2% to 30% with a mean frequency of 8.91 ± 1.63% (**Fig. 2b**). Immunostaining demonstrated that the majority of mCherry signals (red) co-localized with nuclear CDX2 (green, **Fig. 2c**) validating endogenous CDX2 expression. To understand whether CDX2 cells can self-

renew in a similar fashion to stem/progenitor cells, we examined the clonal proliferation of single isolated CDX2 cells for a period of 14 days. CDX2 cells demonstrated a robust clonal efficiency (54.1 ± 6.78%) as analyzed (**Fig. 2d-f**). Interestingly, mCherry-negative chorionic cells also showed the ability of clonal proliferation (44 ± 11.45%) albeit to a lower extent than CDX2 cells. *In vitro* expansion of CDX2 cells showed the retention of mCherry fluorescence through passages (**Fig.2g-i**) with a significant increase in cell yield after each passage until approximately 1 million cells were generated by passage 6 based on input cell number (**Fig.2g**). This suggests that CDX2 cells are amenable to *in vitro* expansion in culture. Response to chemotactic signaling is another key feature of stem/progenitor cells. We examined CDX2 cells for their ability to migrate to chemokine stromal-derived factor 1 α (SDF1) using a transwell migration assay. Before assessing chemotaxis, we preconditioned one group of CDX2 cells with 1uM of AMD3100, an antagonist of SDF1 receptor CXCR4. Under normal conditions, CDX2 cells exhibited a significantly higher migration (22.4 ± 2.68%) to chemokine SDF1 compared to mCherry-negative cells (12.62 ± 2.11%, **Fig.2j**). Despite the presence of SDF1 in the lower well, blocking of CXCR4 using AMD3100 significantly reduced the ability of these cells to migrate. Overall, the chemotaxis response of CDX2 cells was significantly higher and our data show that this ability may be partly mediated via a functional SDF1-CXCR4 axis. In sum, these data demonstrate that CDX2 cells possess key features of stem/progenitor cells as these cells clonally proliferate, are amenable to *in vitro* expansion, and possess significantly higher homing potential *in vitro*.

CDX2 cells possess transcriptomic signatures for cardiovascular development, cell survival, and immune modulation

To decipher the functional repertoire within human placental CDX2 cells, we examined transcript abundance using ultra-low input RNA sequencing. CDX2 is involved in trophectoderm

development leading to trophoblast-mediated placentation, whereas embryonic stem cells are derived from the inner cell mass that significantly downregulated CDX2 expression. Hence, we included an undifferentiated embryonic cell line (hESCs) as a control, along with the mCherry-negative cells which are not enriched for CDX2 at the time of isolation. Using the DESeq2 binomial tool, a comparison of differentially expressed genes (DEGs) showed that approximately 1065 genes were upregulated (154 genes downregulated) in CDX2 cells compared with hESCs. Meanwhile, 46 genes were found to be upregulated (529 genes showing downregulation) in CDX2 cells when compared to mCherry-negative cells (Extended Data Table 1).

The top 30 DEGs across individual samples in a bi-clustering heat map in comparison with hESCs are presented in **Fig. 3a**. The functional pathways in which the differentially expressed genes were involved revealed tissue organization, differentiation, angiogenesis, cell survival, and cardiac development (**Fig. 3b**). The highlighted genes (**Fig. 3a**) upregulated in CDX2 cells (and seen downregulated in hESCs involved TBX3 and NR2F2, which are specifically involved in mesoderm commitment, cardiogenesis, and congenital heart development. The downregulated genes in CDX2 cells involved pluripotency markers, including POU5F1, FOXD3AS1, CLAUDN6, PHC1, and others, as shown in **Fig. 3a**, lowering concerns of tumorigenicity, unlike hESCs or iPSC cells. Gene ontology analyses also corresponded to functions related to immune modulation, and angiogenesis (**Fig. 3b**). Interestingly, migration and chemotaxis are the other key features upregulated in CDX2 cells, which we have functionally demonstrated above.

Examining the transcriptome of mCherry-negative cells further, we noted an upregulated expression of genes involved in immune activation and inflammatory responses. Genes such as RAB44, a member of the Ras family of oncogenes, are involved in immune cell activation. Other immune activation response genes, including EPX, CD80 (a potent immune cell marker in T and

B cell activation), and acute phase genes ORM1, HP, and APOA2 (involved in HDL metabolism and atherosclerotic burden) were upregulated in mCherry-negative cells (**Fig. 3c, d**). Gene ontology analyses showed cardiac and vascular functional features in CDX2 cells (**Fig. 3b**). Vasculogenesis-related genes were differentially expressed in CDX2 cells, especially PECAM1 (CD31). Other genes present included VE-cadherin (CDH5), von Willebrand Factor (vWF), and ACTA2 (**Fig. 3e**), which specify the angiogenic/vascular program. Pathways and genes involved in endothelial-to-mesenchymal (EndMT) transition like SNAI2, KLF4, YAP1, VCAN (Versican), EGFR, CD44, TGFB2, and BMP4 that are implicated in valvular development were found to be significantly upregulated in CDX2mCherry cells when compared with mCherry-negative cells (Extended Data Fig.3). Interestingly, a remarkable cluster of key genes implicated in mesodermal and cardiac commitment (HAND2, DKK1, STC2, FHL1, ITGA, MYOCD, EDN1, and TGFB2) was preferentially upregulated in CDX2 cells (**Fig. 3f**). These gene signatures are implicated in cardiac differentiation and cardiac tissue growth in the fetal and adult heart. CDX2 cells still retained a significant upregulation of mesodermal, cardiac, and sarcomere organization genes, including FHL1, STC2, DKK1, TGFB2, and EDN1 (**Fig. 3f**) in comparison to mCherry-negative cells. These data also suggest that, in comparison to undifferentiated ES cells, chorionic CDX2 cells are farther along the mesodermal/cardiac commitment pathway. These transcriptomics results suggest that CDX2mCherry cells are enriched for a committed cardiovascular gene signature.

CDX2 cells are angiogenic and differentiate into functional endothelial cells

In line with the transcriptome analysis, we also noticed that a subpopulation of CDX2 cells develops endothelial vessel-like structures (27.3±5.6%) and express endothelial markers PECAM1(CD31) and von Willebrand factor (vWF) when co-cultured with murine neonatal cardiomyocytes (**Fig 4a-c**). In addition, under feeder-free conditions, CDX2 cells uniformly

expressed smooth muscle marker (SM22α, 95.5 ± 1.59%) supporting a mesodermal phenotype (**Fig. 4d-e**). To examine functional angiogenesis, we next assessed whether CDX2 cells could form an angiogenic network *in vitro*. Endothelial cells recapitulate angiogenesis by forming capillary-like structures when seeded onto basement membrane-like surfaces such as Matrigel. CDX2 cells displayed tubular extension and loop formation within 3 h and formed endothelial-like networks after 6 h. (**Fig. 4f and g**, **movie S1** https://youtube.com/shorts/0Nnug8eufPQ). mCherry-negative cells displayed a less organized and flattened morphology (**Fig. 4h, i**), of network pattern in comparison to CDX2 cells under identical conditions. HUVEC served as positive control showing a robust tubular network at both 3h and 6h time points (**Fig.4j and k**, **movie S2** https://youtube.com/shorts/xrN6AOsyV5Q?feature=share), while unfractionated chorionic cells did not show any events of tube formation (**Fig. 4l, 4m**). Quantification of the meshes[17] within the endothelial network showed a higher mesh area in CDX2 cells and displayed a higher trend in the branch length, segments, and nodes as noted (**Fig.4 o-s**). Ac-LDL uptake serves as the golden standard of functional endothelium via receptor-mediated endocytosis. Therefore, CDX2mCherry cells primed with endothelial media containing 10ng/mL VEGF were subjected to Ac-LDL for 4 hours and Ac-LDL uptake was confirmed (**Fig 4n**, green). These data suggest that CDX2 cells can undergo endothelial differentiation and form functional endothelium.

CDX2 cells robustly differentiate into spontaneously beating cardiomyocytes

We further examined CDX2 cells for cardiomyogenesis using a neonatal cardiomyocyte feeder system, as described in our murine studies[17]. CDX2mCherry cells from term healthy chorions were plated on beating neonatal murine cardiomyocyte feeders, which provide a niche conducive to differentiation in the absence of additional exogenous growth factors or inducers. Our previous studies successfully used this culture system for proof of concept testing. Isolated

CDX2 cells were plated and monitored on neonatal myocyte feeders. Live cell imaging showed CDX2 cells formed beating organoid-like clusters as early as 4-5 days in culture (**Movie S4** https://www.youtube.com/shorts/XcxbIM8KFtI?feature=share and **Fig. 5a**) Within two weeks, these clusters adhered and spread to display an elongated phenotype while they continued to beat in culture (https://www.youtube.com/shorts/InnTDxkP5Y0?feature=share, (**Fig. 5b** and **Movie S5**). After 4 weeks of culture, immunostaining for human-specific sarcomeric actinin, in combination with cardiac troponin T (cTnT- detect both mouse and human myocytes), demonstrated that CDX2-derived cardiomyocytes robustly expressed cardiac sarcomeric proteins with striations **(Fig. 5c-e'**). On the contrary, the mCherry-negative cells displayed a much lower cardiogenic capacity when cultured in identical conditions, further corroborating our transcriptomics data and supporting cardiogenic ability in CDX2 cells (Extended Data Fig.4). Approximately 71.11±12.15% of input CDX2 cells differentiated into cardiomyocytes (**Fig. 5f**) and these data demonstrate that placental CDX2 cells are cardiogenic and differentiate into spontaneously beating cardiomyocytes in culture. These findings have significant translational implications, as we envision multipotent human placenta-derived CDX2 cells as an innovative approach for cardiovascular regeneration.

Discussion

In this study, we have demonstrated that CDX2-expressing cells isolated from term human placenta possess key characteristics of stem/progenitor cells and differentiate into cardiovascular lineages in addition to migrating to the chemokine SDF1α. CDX2 is essential in embryonic development and is found in the trophectoderm, which in turn regulates placentation. During embryonic development, the placenta and fetal heart progress in parallel (placenta-heart axis) with the placenta regulating fetal cardiomyocyte proliferation, signifying a key functional association

between these organs[8-10]. Our current findings lend credence to such a scenario as placenta-derived CDX2 cells are uniquely poised to drive cardiovascular commitment and can now be viewed as a cellular target for cardiogenesis.

Various cell sources for therapeutic approaches have been studied in cardiac regeneration for decades, and the safety of such approaches has been established in clinical trials. However, finding an ideal and easily accessible cell type that can give rise to cardiovascular cells, aside from ESCs and iPSC, has proven difficult. Prenatal placental cells, particularly placental mesenchymal stem cells (PMSCs) and amniotic epithelial cells (AECs) have anti-inflammatory, angiogenic, and paracrine mechanisms that are beneficial for cardiac regenerative approaches but have not been shown to generate *de novo* cardiomyocytes[18-20]. On the other hand, endogenous trophoblast progenitors in the placenta have not been widely explored for their differentiation into other cell types. Our previous studies demonstrated the potential of murine Cdx2 lineage cells in the placenta to migrate to the sites of cardiac injury and produce new cardiovascular cells, significantly improving cardiac function[16]. The current study emphasizes the direct translational significance as multipotent human CDX2 cells are retained in the cytotrophoblast of the human placenta until term. Our observation of the localization of CDX2 to the cytotrophoblast region is consistent with the studies on the early-gestational placenta[21]. In addition, CDX2 was also found to be expressed in cells derived from the term human placentas[22]. Cytotrophoblast cells are proliferative stem cells that migrate and invade maternal spiral arteries during placentation. Similarly, we observed that CDX2 cells from term placenta, expressed villous trophoblast markers, exhibit clonal proliferation and migration supporting the stem/progenitor characteristics suitable for cardiac regenerative approaches.

CDX2 cells and mCherry-negative cell populations were examined in our studies using a lentivirus-based isolation method. Even though sourced from healthy placentas, differences in proliferation among various samples existed. We are presently targeting the kinetics of proliferation and differentiation at the single-cell level will further provide valuable clues that can resolve cellular heterogeneity within placenta samples. In this study, we have also incorporated a sizable group of healthy donors of varied races which included 106 placentas, to account for any biological diversity. This approach may facilitate a more inclusive analysis as the placenta samples are representative of a broader population. The selection of cells that were CDX2mCherry positive also made it easier to study the functional competency of mCherry-negative counterparts from the same anatomical region of the chorion. Even though clonal efficiency was not drastically different, with this closer comparison, we could conclusively determine that CDX2 cells have enhanced cardiovascular capability compared with mCherry-negative cells. Similarly, the transcriptomic signature of mCherry-negative cells displayed a lesser extent of mesodermal differentiation when compared to CDX2 cells. With the additional hESC stem cell control, we also observed that CDX2 cells significantly upregulated chemotaxis, migration, and cardiovascular gene signatures in both comparisons.

Consistent with transcript analyses, human CDX2 cells generated spontaneously beating cardiomyocyte cell clusters within 5 days followed by approximately 70% of CDX2 cells differentiating into cardiomyocytes on neonatal murine cardiomyocyte feeder. Remarkably, the time frame for the emergence of beating clusters was relatively shorter in CDX2 cells contrary to other inductive co-culture approaches or standard protocols using pluripotent stem cells, which demonstrate the onset of beating within 8–12 days[23-25]. It is conceivable that this is because of the enriched pre-existing cardiogenic transcriptome present in the isolated CDX2 cells. These findings

suggest that CDX2 cells may be a promising population for generating cardiomyocytes in a shorter time frame, which could have significant implications for regenerative medicine.

Since the placenta becomes an increasingly vascular organ during the course of gestation, cells from the placenta can be highly angiogenic. As we noted from the data from our trancriptomic analyses, endothelial tube formation from CDX2 cells suggested a strong angiogenic commitment and Ac-LDL uptake confirmed that the CDX2-derived endothelial cells are functional. Angiogenesis is a crucial feature in cell therapy and cardiac repair, as the engraftment of adoptively transferred cells into the surrounding microenvironment is highly dependent on establishing *de novo* vasculature. Interestingly, angiogenesis and the invasive nature of trophoblast cells are interlinked as the migration potential of trophoblast cells directs endothelialization/angiogenesis during placentation[26,27]. On the other hand, SDF1-mediated chemotaxis is further involved in stem cell-mediated homing for regeneration[28-30] and CDX2 cells demonstrated significantly higher SDF1-mediated migration compared to our two control populations. Our findings demonstrate the functional competency of CDX2 cells in several scenarios, making them a promising cell population for further therapeutic applications.

The most exciting outcome of these studies is that a new progenitor cell type has been identified from a limitless source (term placenta) that differentiates into spontaneously beating cardiomyocytes as well as functional vascular cells *in vitro*, thus providing a foundation for more precision-guided clinical trials of cardiac regeneration.

References

1 Trounson, A. & McDonald, C. Stem Cell Therapies in Clinical Trials: Progress and Challenges. *Cell Stem Cell* **17**, 11-22, doi:10.1016/j.stem.2015.06.007 (2015).

2 Xin, M., Olson, E. N. & Bassel-Duby, R. Mending broken hearts: cardiac development as a basis for adult heart regeneration and repair. *Nat Rev Mol Cell Biol* **14**, 529-541, doi:10.1038/nrm3619 nrm3619 [pii] (2013).

3 Martinez, J., Zoretic, S., Moreira, A. & Moreira, A. Safety and efficacy of cell therapies in pediatric heart disease: a systematic review and meta-analysis. *Stem Cell Res Ther* **11**, 272, doi:10.1186/s13287-020-01764-x (2020).

4 Cambria, E. *et al.* Translational cardiac stem cell therapy: advancing from first-generation to next-generation cell types. *NPJ Regen Med* **2**, 17, doi:10.1038/s41536-017-0024-1 (2017).

5 Sultana, N. *et al.* Resident c-kit(+) cells in the heart are not cardiac stem cells. *Nat Commun* **6**, 8701, doi:10.1038/ncomms9701 (2015).

6 Li, Y. *et al.* Genetic Lineage Tracing of Nonmyocyte Population by Dual Recombinases. *Circulation* **138**, 793-805, doi:10.1161/CIRCULATIONAHA.118.034250 (2018).

7 He, L., Nguyen, N. B., Ardehali, R. & Zhou, B. Heart Regeneration by Endogenous Stem Cells and Cardiomyocyte Proliferation: Controversy, Fallacy, and Progress. *Circulation* **142**, 275-291, doi:10.1161/CIRCULATIONAHA.119.045566 (2020).

8 Burton, G. J. & Jauniaux, E. Development of the Human Placenta and Fetal Heart: Synergic or Independent? *Front Physiol* **9**, 373, doi:10.3389/fphys.2018.00373 (2018).

9 Mahadevan, A., Tipler, A. & Jones, H. Shared developmental pathways of the placenta and fetal heart. *Placenta*, doi:10.1016/j.placenta.2022.12.006 (2022).

10 Ward, E. J. *et al.* Placental Inflammation Leads to Abnormal Embryonic Heart Development. *Circulation*, doi:10.1161/CIRCULATIONAHA.122.061934 (2022).

11 Shen, H. *et al.* Extracardiac control of embryonic cardiomyocyte proliferation and ventricular wall expansion. *Cardiovasc Res* **105**, 271-278, doi:10.1093/cvr/cvu269 (2015).

12 Antoniadou, E. & David, A. L. Placental stem cells. *Best Pract Res Clin Obstet Gynaecol* **31**, 13-29, doi:10.1016/j.bpobgyn.2015.08.014 (2016).

13 Maltepe, E., Bakardjiev, A. I. & Fisher, S. J. The placenta: transcriptional, epigenetic, and physiological integration during development. *J Clin Invest* **120**, 1016-1025, doi:10.1172/JCI41211 (2010).

14 Niwa, H. *et al.* Interaction between Oct3/4 and Cdx2 determines trophectoderm differentiation. *Cell* **123**, 917-929, doi:10.1016/j.cell.2005.08.040 (2005).

15 Kara, R. J. *et al.* Fetal cells traffic to injured maternal myocardium and undergo cardiac differentiation. *Circ Res* **110**, 82-93, doi:10.1161/CIRCRESAHA.111.249037 CIRCRESAHA.111.249037 [pii] (2012).

16 Vadakke-Madathil, S. *et al.* Multipotent fetal-derived Cdx2 cells from placenta regenerate the heart. *Proc Natl Acad Sci U S A* **116**, 11786-11795, doi:10.1073/pnas.1811827116 (2019).

17 Carpentier, G. *et al.* Angiogenesis Analyzer for ImageJ - A comparative morphometric analysis of "Endothelial Tube Formation Assay" and "Fibrin Bead Assay". *Sci Rep* **10**, 11568, doi:10.1038/s41598-020-67289-8 (2020).

18 Gorodetsky, R. & Aicher, W. K. Allogenic Use of Human Placenta-Derived Stromal Cells as a Highly Active Subtype of Mesenchymal Stromal Cells for Cell-Based Therapies. *Int J Mol Sci* **22**, doi:10.3390/ijms22105302 (2021).

19 Song, Y. S. *et al.* Transplanted Human Amniotic Epithelial Cells Secrete Paracrine Proangiogenic Cytokines in Rat Model of Myocardial Infarction. *Cell Transplant* **24**, 2055-2064, doi:10.3727/096368914X685609 (2015).

20 Roy, R. *et al.* Cardioprotection by placenta-derived stromal cells in a murine myocardial infarction model. *J Surg Res* **185**, 70-83, doi:10.1016/j.jss.2013.05.084 (2013).

21 Soncin, F. *et al.* Comparative analysis of mouse and human placentae across gestation reveals species-specific regulators of placental development. *Development* **145**, doi:10.1242/dev.156273 (2018).

22 Shablii, V. *et al.* High Proliferative Placenta-Derived Multipotent Cells Express Cytokeratin 7 at Low Level. *Biomed Res Int* **2019**, 2098749, doi:10.1155/2019/2098749 (2019).

23 Lian, X. *et al.* Robust cardiomyocyte differentiation from human pluripotent stem cells via temporal modulation of canonical Wnt signaling. *Proc Natl Acad Sci U S A* **109**, E1848-1857, doi:10.1073/pnas.1200250109 (2012).

24 Balafkan, N. *et al.* A method for differentiating human induced pluripotent stem cells toward functional cardiomyocytes in 96-well microplates. *Sci Rep* **10**, 18498, doi:10.1038/s41598-020-73656-2 (2020).

25 Mummery, C. L. *et al.* Differentiation of human embryonic stem cells and induced pluripotent stem cells to cardiomyocytes: a methods overview. *Circ Res* **111**, 344-358, doi:10.1161/CIRCRESAHA.110.227512 (2012).

26 Piera-Velazquez, S. & Jimenez, S. A. Endothelial to Mesenchymal Transition: Role in Physiology and in the Pathogenesis of Human Diseases. *Physiol Rev* **99**, 1281-1324, doi:10.1152/physrev.00021.2018 (2019).

27 Alvandi, Z. & Bischoff, J. Endothelial-Mesenchymal Transition in Cardiovascular Disease. *Arterioscler Thromb Vasc Biol* **41**, 2357-2369, doi:10.1161/ATVBAHA.121.313788 (2021).

28 Lapidot, T. & Kollet, O. The essential roles of the chemokine SDF-1 and its receptor CXCR4 in human stem cell homing and repopulation of transplanted immune-deficient NOD/SCID and NOD/SCID/B2m(null) mice. *Leukemia* **16**, 1992-2003, doi:10.1038/sj.leu.2402684 (2002).

29 Lau, T. T. & Wang, D. A. Stromal cell-derived factor-1 (SDF-1): homing factor for engineered regenerative medicine. *Expert Opin Biol Ther* **11**, 189-197, doi:10.1517/14712598.2011.546338 (2011).

30 Song, M. *et al.* Regeneration of chronic myocardial infarction by injectable hydrogels containing stem cell homing factor SDF-1 and angiogenic peptide Ac-SDKP. *Biomaterials* **35**, 2436-2445, doi:10.1016/j.biomaterials.2013.12.011 (2014).

Main Figure Legends

Figure 1: CDX2 expression found to be enriched in term human chorionic tissues. (a) CDX2 mRNA expression in the first-trimester chorionic villous sample and term chorion from the healthy placenta. L=DNA ladder (Gene Ruler ultralow DNA ladder). Human adenocarcinoma cell line DLD1 displays a higher expression of CDX2 and hence served as a positive control. Gapdh served as an internal control. (b) Western blot analyses on term healthy chorionic samples (80µg protein/sample) showed CDX2 protein (40KDa) with a doublet pattern indicative of the alternate splicing. DLD1 served as a positive control, while HeLa cells as a control with low endogenous CDX2 expression. (c) Immunofluorescence detection of CDX2 in term chorion showed that CDX2 (clone CDX88-red) is mainly expressed in the villi region encompassing the cytotrophoblast cells

and co-express trophoblast marker Cytokeratin 7 (pink -CKT7). (d) Quantification of tissue sections showing the percentage of CDX2 cells co-expressing CKT7. (e) Approximately 50% (50.5±5.0%) of CDX2 cells co-expressed HLA-G, a crucial marker identifying extravillous trophoblast progenitors in the placenta. n=3 independent placental samples wherein 3 different ROIs from each section were screened.

Figure 2: CDX2 cell isolation, proliferation, and homing *in vitro* (a) CDX2 lenti mCherry was used to transduce chorionic cells (50 MOI), and cells expressing CDX2 displayed mCherry fluorescence. (b) Flow cytometry-based isolation of mCherry+ cells and quantification of CDX2mCherry cells from various placentas. Data are presented as mean ± SEM (n=25 independent samples). (c) The specificity of the lentivirus-based selection of CDX2 cells was validated using CDX2mAb (CDX-88clone). Co-localization of mCherry fluorescence with CDX2 antibody (Alexa 488) and trophoblast marker Cytokeratin 7 (CKT7-pink is shown (d,e) Representative phase contrast image showing clonal proliferation CDX2 cells on day 14 (e) compared to day 1 (d) in culture. (f) Clonal efficiency was analyzed on day 14 and found to be 54.1 ± 6.78% in CDX2 cells versus 44 ± 11.45% in mCherry negative cells. Data are presented as mean ± SEM (n=4 independent samples) (g) Quantification of mCherry cells after expansion showed a significant increase of up to 1 million cells by passage 6 compared to day 0 of isolation, Data represented as mean±SEM (n=3, *p<0.05, **p<0.01) (h) Retention of mCherry expression over the various passages as analyzed by flow cytometry and (i) a representative image at p5. (j) In vitro homing of CDX2 cells and mCherry negative cells to chemokine SDF1 is dependent on the CXCR4 axis. CDX2 cells show significantly higher migration in both conditions compared to mCherry-negative cells. Data are presented as mean ± SEM (n=3 biological replicates comprising 3 independent samples *p<0.05, **p<0.01)

Figure 3: Ultra-low input RNAseq analyses on CDX2 cells versus hESCs and mCherry negative cells (a) Bi-clustering heat map showing the expression profile of the top 30 differentially expressed genes in CDX2 cells (labeled 1-5 right) versus hESCs (H9 ES ctrl pooled extreme left). Genes were sorted by their adjusted p-value by plotting the log2 transformed expression values. The yellow-green color code indicates the upregulated and the blue-gray color code indicates the downregulated genes across the samples. CDX2 cells showed upregulated mesoderm commitment genes including NR2F2 and TBX3 (cardiogenic) while downregulating pluripotent markers CLDN6, POU5F1, ESRG (b) Further, differentially expressed genes (up to 40) vs. hES cells show gene ontology terms enriched with an adjusted p-value less than 0.05 corresponding to functions related to angiogenesis, immune modulation, migration, and chemotaxis. (c) A bi-clustering heat map with the top 30 differentially expressed genes showing the upregulated function of inflammatory response and immune genes in mCherry negative cells (n=4 independent samples in each group) (d) GO analyses demonstrated upregulation of functional pathways including T cell proliferation, MHC class II antigen processing, and presentation, IFN gamma mediated signaling, and cholesterol biosynthesis in mCherry negative cells. (e,f) CDX2 cells displayed enriched transcriptomes reflecting cardiovascular development. Vascular genes like PECAM1, VE-cadherin *(*CDH5*),* and smooth muscle actin *(*ACAT2*)* were upregulated in CDX2 cells in comparison to hES cells and mCherry negative control samples. (f) Genes associated with cardiac development including HAND2, DKK1, STC2, FHL1, ITGA1, MYOCD EDN1, and TGFB2 showed preferential upregulation in CDX2 cells.

Figure 4: CDX2 cells are angiogenic and display endothelial tube formation *in vitro* (a) Subset of CDX2mCherry cells (red) expressed vascular lineage marker CD31 (pink) and further gave rise to blood vessel-like assembly (and stained positive for endothelial marker von Willebrand Factor

(vWF-green) upon co-culture with neonatal cardiomyocytes (b, c). Data represented as mean±SEM of four independent samples (n=4). (d,e) CDX2mCherry cells also expressed smooth muscle marker SM22α upon feeder-free culture using IMDM+10%FBS (f,g) Endothelial tube formation by CDX2mCherry cells on matrigel in 3hrs and the formation of endothelial-like networks within 6hrs, also refer to movie S1.(h, i) mCherry negative cells showing networks albeit not as intact and optimal as their CDX2mCherry counterpart on matrigel. (j,k) Human umbilical vein endothelial cells (HUVEC) served as a positive control, also refer to movie S2 (l,m) Total chorionic cells from the placenta did not exhibit endothelial tube formation at both time points. (n) Ac-LDL (Alexa-488) uptake by primed (M200 medium +LSGS+ 10ng/mL VEGF) CDX2mCherry cells suggesting the formation of a functionally active endothelium (o-s) Quantification of the endothelial network using ImageJ software with angiogenesis analyzer showed a higher endothelial loop like area, branching segments compared to mCherry negative cells (n=5 independent CDX2mCherry positive and n=2 independent mCherry negative samples with biological triplicates per assay.)

Figure 5: CDX2 cells differentiate into spontaneously beating cardiomyocytes in co-culture with neonatal myocyte feeder (a) Snapshot of a beating CDX2mcherry cell cluster on day 5 on co-culture with murine neonatal cardiomyocytes feeder (non-mCherry-gray cells in the background), also see movie S3. (b) Snapshot of beating adhered and elongated CDX2mCherry cardiomyocytes 3 weeks in culture (movie S4). (c) Most of the CDX2mCherry cells-derived cardiomyocytes (mCherry-red) stain positive for human cardiac sarcomeric actinin (pink-Alexa 647) and cardiac troponin T (cTnT-green Alexa 488). The specificity of the human actinin antibody was detected by a lack of staining on murine feeder myocytes in the background, while cTnT (green) detects both mouse and human cardiomyocytes. Yellow box 1 is further highlighted

to the right (d and d') showing the striated sarcomeres visible on human CDX2 mCherry-derived cardiomyocytes (actinin pink + cTnT green+). Meanwhile, green box 2 and the expanded panels point to the endogenous murine feeder myocyte that expresses only cTnT (green) (e and e'). Nuclei are counterstained using DAPI (blue). (f) Quantification revealed that approximately 71.11±12.15% of input CDX2 cells differentiated into cardiomyocytes as shown. Data are represented as mean ± SEM (n=5 independent samples).

Methods

Human subjects

Pregnant women enrolled in this study ranged from to 18-45 years, were ethnically and racially diverse, and reflected those served by the Maternal Fetal Medicine Practice at Mount Sinai. 189 patients are currently enrolled in this study. Placenta samples were collected under two cohorts. 1) Mount Sinai approved IRB protocol (Study 20-0068, IF2646084), which reflects the prospective cohort that has now 189 enrolled patients (including future due dates) from which 31 samples were collected thus far based on the viable delivery window (weekdays 9-5 pm). Cohort 2, the de-identified cohort, contained 75 fresh tissue samples under the auspices of the Institutional Biobank at Mount Sinai Pathology Core facility. De-identified samples (all identifying patient information was replaced by a BRP #ID) at the Biorepository Core Facility were sampled by a neonatal placental pathologist. Both sample collections followed the standard protocol in order not to interfere with any needed clinical assessment of the placenta and to only obtain tissue that would otherwise be discarded. Unless otherwise mentioned, each experiment was performed with at least three different patient samples (n=3).

Placental CDX2 cell isolation

Placentas were received within 30 min-120 min of delivery. Gross appearance was briefly examined, including identification of the cord insertion site and disc edges. Approximately 5.0 x 2.0 cm rectangular area of each full-thickness disc was incised off by a surgical blade midway from the cord insertion site and the disc edge, avoiding obvious sub-chorionic fibrin deposition. Any remaining amnion was removed using forceps. Finally, the decidual surface was shaved using a blade to minimize the maternal component. The chorionic tissue was then quickly transferred to 1X Hanks Balanced Salt Solution (HBSS) containing 2X penicillin and streptomycin and kept on ice. The fresh tissue was rinsed thoroughly using 1X HBSS to remove blood, minced into approximately $1mm^3$, pieces, and transferred to 50mL falcon conical tubes containing 2 mg/mL Collagenase Type 2 (Worthington, NJ, Cat#LS0004194) and 1 mg/mL Pronase (Calbiochem,Cat#53702) solution in 1X HBSS. The samples were incubated in enzyme solution for 2 h at 37 °C and 5% CO_2. The tissue mixture containing the enzyme solution was gently mixed every 20 min using disposable pipettes to facilitate digestion. At the end of digestion, the enzyme reaction was stopped by the addition of serum, and the cell mixture was filtered using a 100-micron cell strainer (Falcon, Cat#352360) and centrifuged at 1600rpm for 4 min. Red blood cells were removed using 1X RBC lysis buffer (10X stock, eBioscience, Cat# 00-4300-54) by incubating the cell pellet in lysis buffer (15 min, room temperature in the dark) followed by centrifugation. The final cell pellet was resuspended in IMDM+10% FBS or the respective assay medium for downstream experiments.

Lentiviral transduction and isolation of placental CDX2 cells

To select viable CDX2 cells from the total chorionic cells, we designed a lentiviral construct in which the human CDX2 promoter drives mCherry fluorescence. The CDX2 gene is oriented in the reverse (3’-5’) sequence, and its promoter expression is not as strong as that of conventional

upstream promoters. Hence, we designed three different constructs using sequences spanning different regions upstream of the 3' UTR, and in some cases, also spanning a fragment into the start codon to include promoter region 1 (612bps), promoter region 2 (1174bps), and promoter region 3 (1197bps). The downstream detection is by mCherry fluorescence and a ubiquitous CMV promoter with the same vector backbone served as a control for transduction efficiency. The human adenocarcinoma cell line, DLD1, served as a positive control for CDX2. Based on the validation experiments (Extended Data Fig.2), CDX2 promoter 1 displayed the strongest mCherry fluorescence; hence, we used lentiCDX2 (612bps) for all experiments. For transduction, chorionic cells were plated at a density of 10^5 cells/24 well in IMDM+10% FBS and were allowed to adhere overnight. The following day, cells were transduced with lentivirus at 50 multiplicity of infection (MOI=50) viral particles per cell with8µg/mL polybrene to facilitate transduction. The plates were spinoculated at 2000 rpm for 1 min and incubated at 37 °C and 5% CO_2 for 48 -72h After 48 h, the medium was replaced and the cells were examined for mCherry fluorescence under a Zeiss AxioObserver epifluorescence microscope; mCherry-positive and mCherry-negative populations were separated using flow cytometry-based sorting using a BD Influx/IMI5L/Cytek Aurora sorter.

Ultralow-input RNA sequencing

Isolated CDX2mCherry cells (n=5) mCherry negative cells (n=4) and hES cells (n=2 pooled) were centrifuged and 200uL Tri reagent (Thermo Fisher Scientific, USA) was added and incubated at room temperature for 15 min. The samples were stored at -80°C until RNA extraction and library preparation were performed. The library preparation workflow is depicted below for sequencing on Illumina Hiseq (HiSeq™ 2000 Sequencing System, Illumina, Genewiz/Azenta Life Sciences).

Statistical Analysis

The number of biological and technical replicates is indicated in figure legends wherever appropriate. Data are presented as mean ± SEM unless otherwise indicated. All immunohistochemistry micrographs were quantified by ImageJ (analyze particle). For pairwise comparisons, significance was determined followed by post-hoc Tukey's or Bonferoni's test to conserve the inflation of the Type I error rate. An unpaired t-test was used to analyze the rest of the datasets. A two-tailed alpha level of 0.05 was used, and a P value of ≤ 0.05 was considered significant.

Acknowledgments

We thank Ms. Carolyn Quinn for proofreading the manuscript. We thank the Flow Cytometry Core Facility, Imaging Core Facility, Biorepository and Pathology Core Facility, and Stem Cell Engineering Core at the Icahn School of Medicine at Mount Sinai for technical assistance. We thank Dr. Lisa Edelman (Genetics and Genomics Sciences, Mount Sinai) for kindly providing chorionic villous samples for the study. This study was supported by New York Stem Cell Board funds IIRP Contract C32608GG, NIH/NHLBI R01HL150345 to H.W.C and KL2 1KL2TR004421-01(NIH CTSA Mount Sinai) to SVM.

Author Contributions

S.V.M., designed and performed experiments, analyzed the data and wrote the paper. B.J.W. performed experiments, analyzed the data, and organized the figures. M.O., coordinated the enrollment, assisted in the processing of placental samples, and performed cell cultures. F.D. examined the placenta and performed the sampling. R.B. examined the de-identified patient data and provided the tissue sections. S.G. and R.S. were closely involved in coordinating the human subject enrollment and assisted in the timely procurement of samples. H.W.C. conceived the study,

interpreted the results with all authors, and wrote the paper with S.V.M. All authors edited and approved the paper.

Competing Interest Declaration

H.W.C the senior and co-corresponding author of this study is the inventor of an issued EU patent and pending US patent owned by Icahn School of Medicine at Mount Sinai (Methods of Cardiac Repair, No. 12847330.3) regarding the use of CDX2 cells for heart repair. She is also the founder of a biotech VentriNova, Inc. that may benefit from the publication of the results presented regarding human CDX2 cells. Although the company is still in the early stages and seeking institutional financing, H.W.C. owns stock in the company.

Additional Information

Supplementary Information is available for this paper. Online-only methods are available for this paper. Correspondence and requests for materials should be addressed to Hina Chaudhry at hina.chaudhry@mssm.edu

Data and code availability

The new plasmids generated in this study will be made available upon publication. No unique reagents were generated from this study. Bulk sequencing data will be made available in the NCBI Sequencing Read Archive (SRA). De-identified placental information along with the patient's age and race/ethnicity data will be available upon request.

Extended Data Figure Legends

Extended Data Figure 1. CDX2-expressing cells are enriched in chorionic cells in human term placenta (a) Chorionic tissue sections show nuclear CDX2, especially in the villous region and within the cytotrophoblast, whereas amniotic tissue sections (b) showed low/lack CDX2 (red-mAb Abcam CDX88-clone) expression. Images represent immunostaining from two different

placentas samples. (c) De-identified human colon tumor tissue sections served as positive control and displayed a higher CDX2 expression.

Extended Data Figure 2. Human CDX2 promoter-driven lentivirus approach (a-c) Vector map incorporating different sequence lengths of huCDX2 promoters in the vector backbone. selected promoter 1 (CDX2 612bps) designed to incorporate sequences spanning upstream exon 1 ~300 sequences and further ~308 bps into exon 1 right before the first open reading frame (ORF) at the start codon ATG site. All vector maps containing mCherry are inserted at the ORF as a fluorescence-based readout that reflects the activity of the promoter. (d-g) Human adenocarcinoma cell line DLD1 displays a higher expression of endogenous CDX2 and hence we assessed the efficiency of the designed promoters in detecting CDX2 by visualizing the mCherry fluorescence in DLD1. The plasmid vector showing Promoter 1 (e) showed an optimal mCherry readout. (h-l) Lenti CMV mCherry showed an increase in mCherry fluorescence as MOI was increased from 5-100. (m-q) In a similar manner, CDX2 lenti mCherry (promoter 1) was used and 50MOI was chosen further for the selection of CDX2-expressing cells from the term placenta.

Extended Data Figure 3 : Upregulated EndoMT/EMT transcriptome in CDX2 mCherry cells (a,b) CDX2mCherry cells show upregulated markers implicated in the endothelial-mesenchymal transition, crucial for valve formation during cardiac development. Mean normalized values are plotted in the Y-axis and Log2 fold change in comparison to mCherry negative cells are annotated above each CDX2 bar graph (n=4)

Extended Data Figure 4. Limited cardiac differentiation of mCherry negative cells on neonatal cardiomyocytes feeder (a) and (c) are representative immunofluorescence images from two different mCherry negative placenta cells on murine neonatal cardiomyocytes feeder. mCherry negative cells did not efficiently differentiate and did not show cTnT (detects both mouse and

human cardiomyocytes) expression, however, weakly expressed human-specific actinin (pink-not detected in mouse myocytes). Panel (b) represent the highlighted field from overlay (a) showing human-specific actinin (pink) that only detects human myocytes whereas panel b' shows the endogenous murine cTnT (green) expression. Similarly, panel (d) represents the highlighted field from overlay image (c) representing mCherry negative cell-derived cell expressing human-specific actinin (pink), whereas cTnT (green) detects murine cardiomyocyte within the feeder.

Figure 1

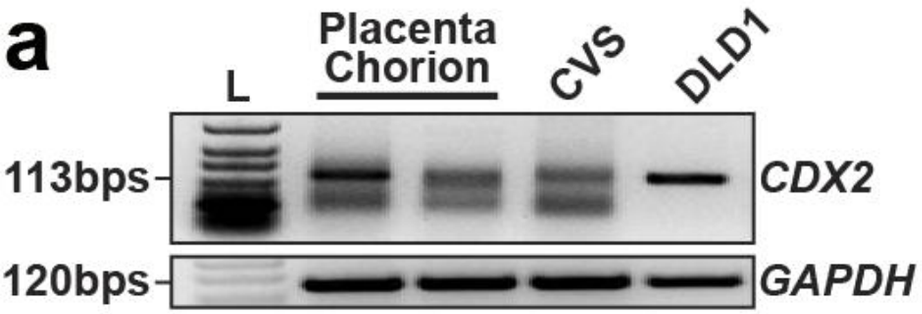
a
L
Placenta Chorion
CVS
DLD1
113bps
120bps
CDX2
GAPDH

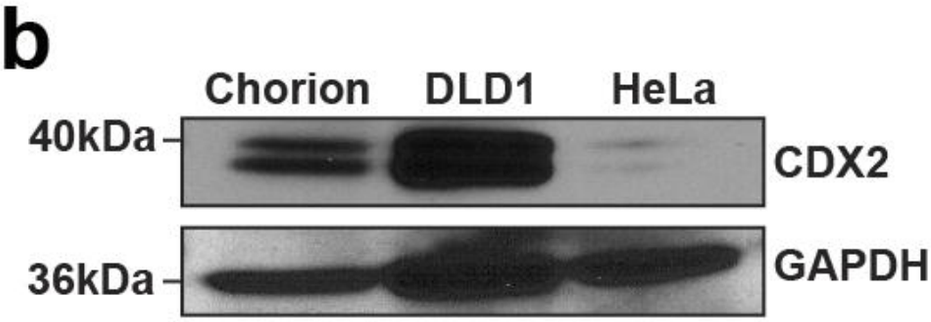
b
Chorion
DLD1
HeLa
40kDa
36kDa
CDX2
GAPDH

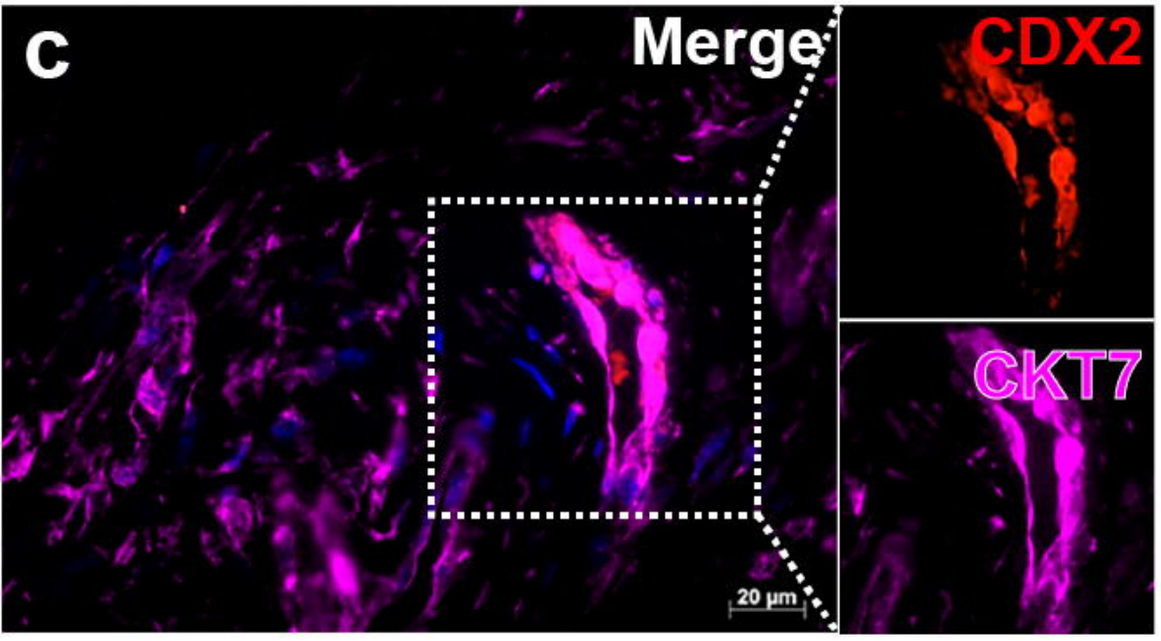
c
Merge
CDX2
CKT7
20 µm

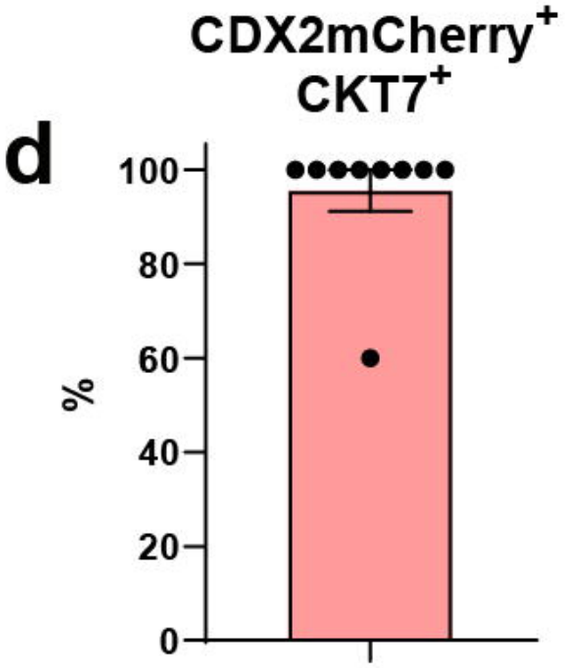
d
CDX2mCherry+
CKT7+
%
100
80
60
40
20
0

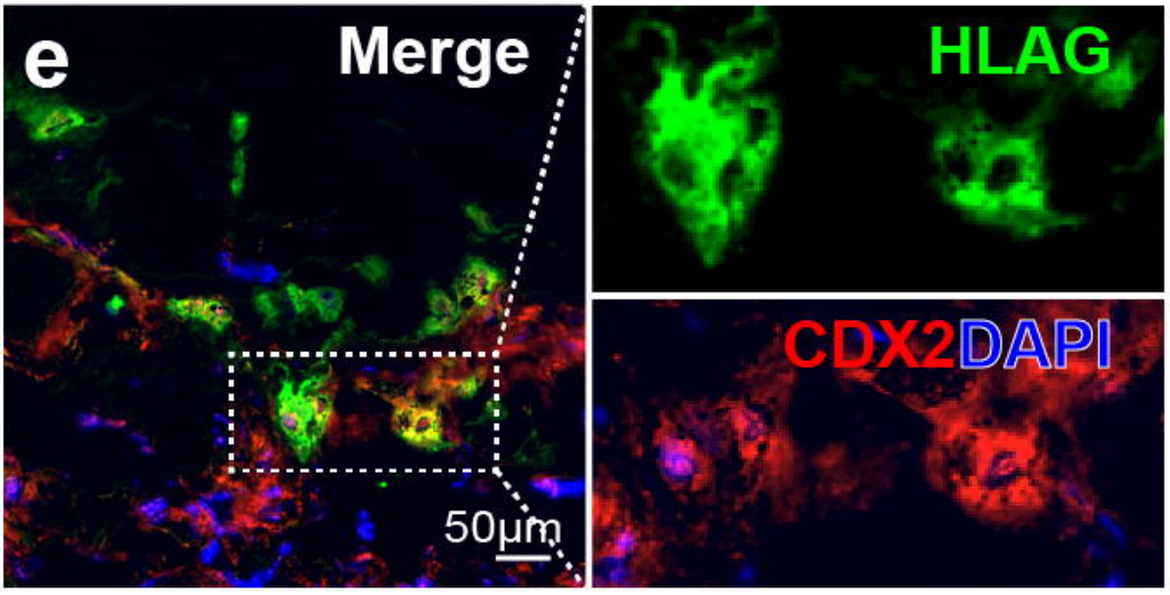
e
Merge
HLAG
CDX2DAPI
50µm

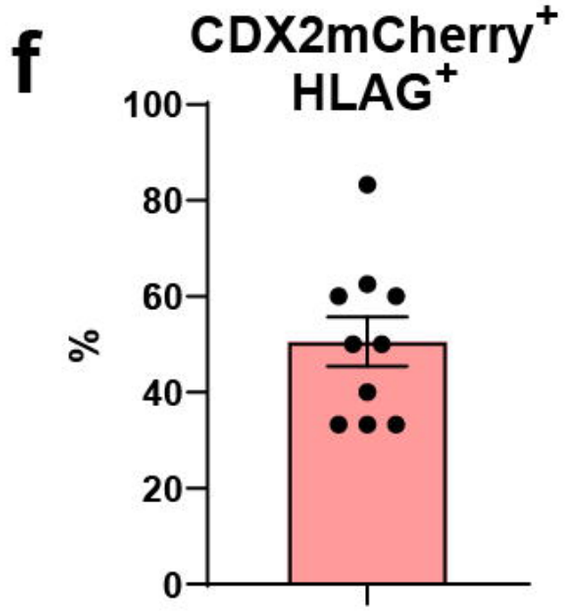
f
CDX2mCherry+
HLAG+
%
100
80
60
40
20
0

Figure 2

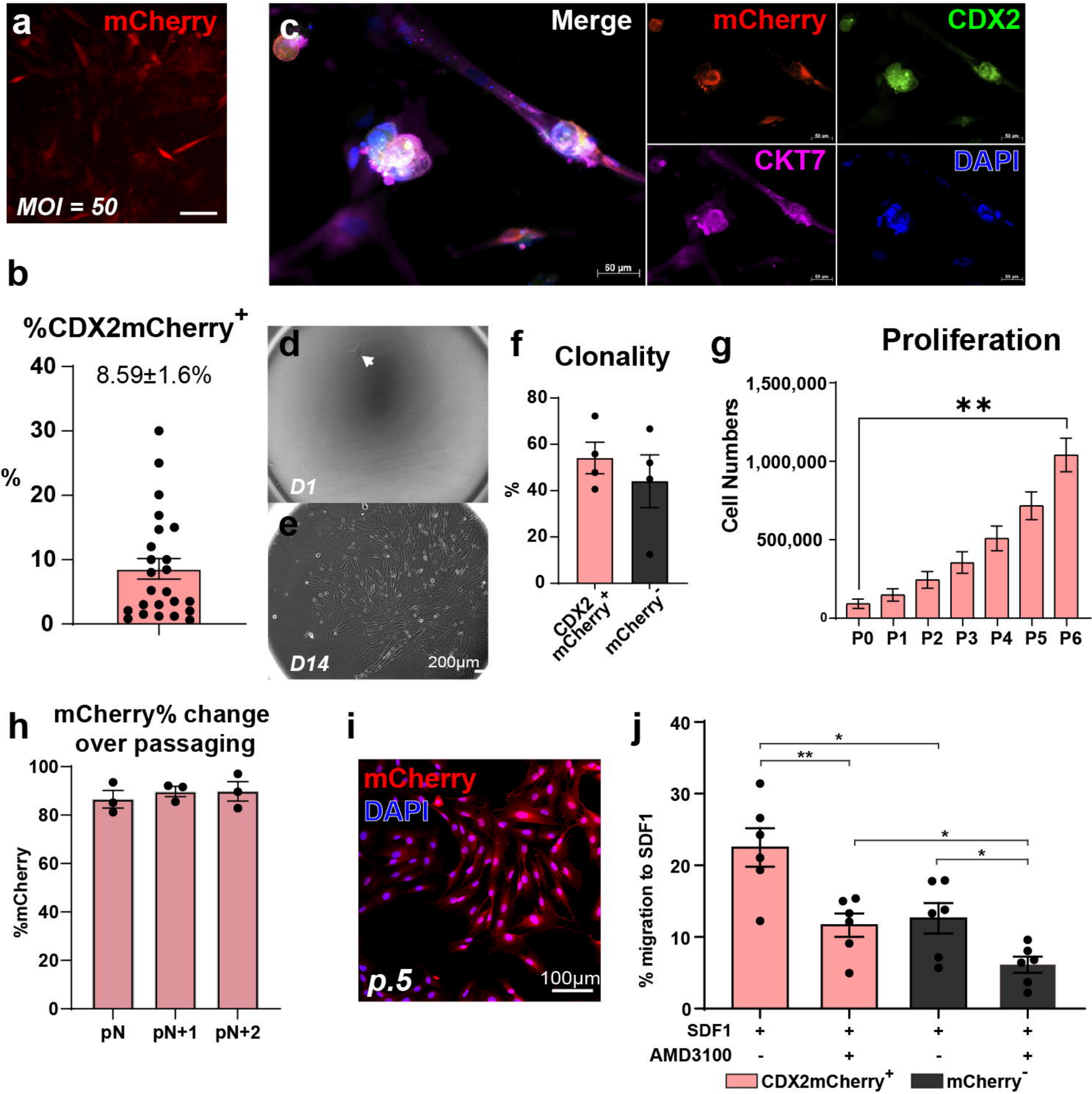
a
mCherry
MOI = 50
c
Merge
50 µm
mCherry
CDX2
CKT7
DAPI
b
%CDX2mCherry+
8.59±1.6%
%
d
D1
e
D14
200µm
f
Clonality
%
CDX2 mCherry+
mCherry-
g
Proliferation
Cell Numbers
**
P0
P1
P2
P3
P4
P5
P6
h
mCherry% change over passaging
%mCherry
pN
pN+1
pN+2
i
mCherry
DAPI
p.5
100µm
j
% migration to SDF1
SDF1
AMD3100
CDX2mCherry+
mCherry-

Figure 3

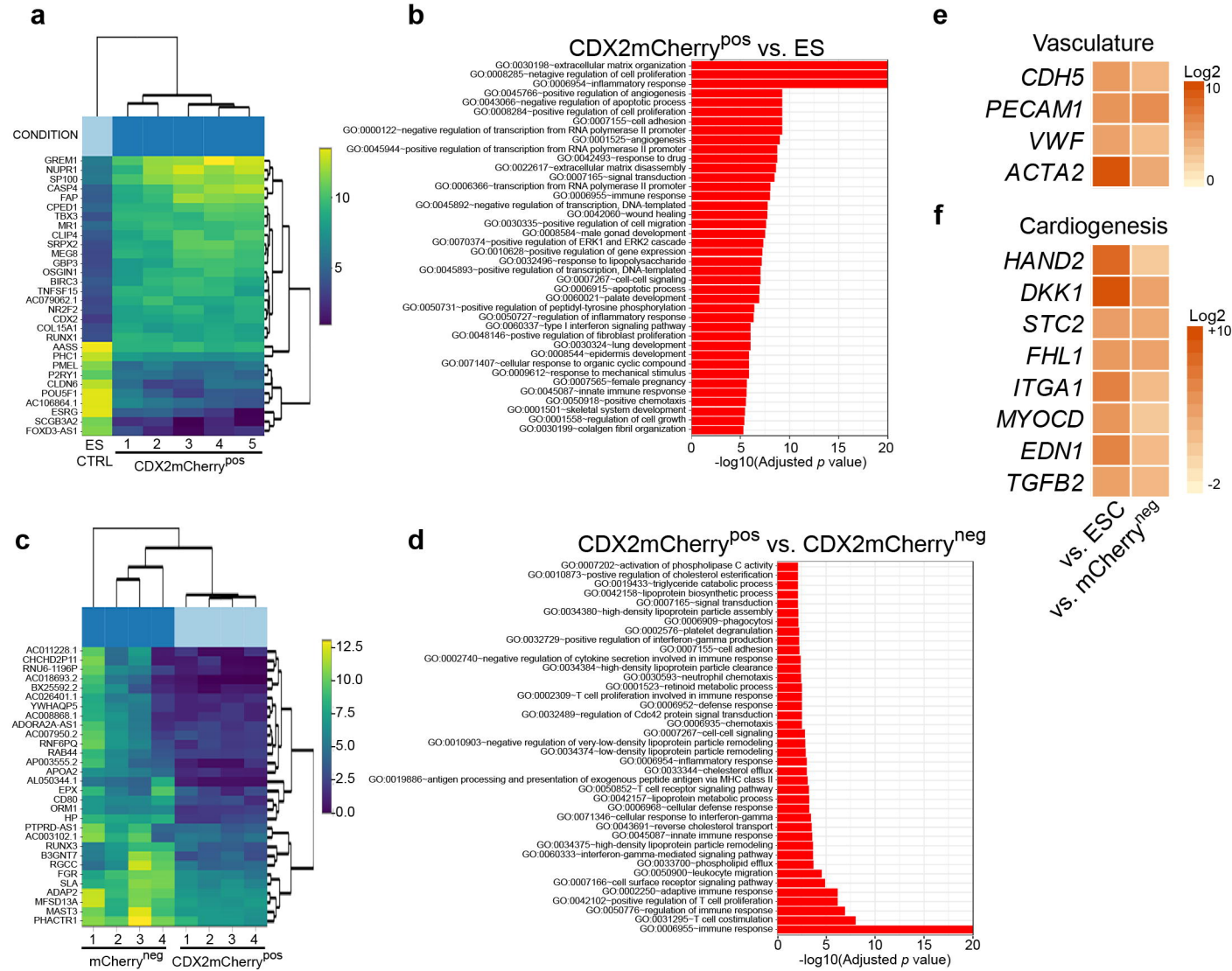
a
CONDITION
GREM1
NUPR1
SP100
CASP4
FAP
CPED1
TBX3
MR1
CLIP4
SRPX2
MEG8
GBP3
OSGIN1
BIRC3
TNFSF15
AC079062.1
NR2F2
CDX2
COL15A1
RUNX1
AASS
PHC1
PMEL
P2RY1
CLDN6
POU5F1
AC106864.1
ESRG
SCGB3A2
FOXD3-AS1
10
5
ES
CTRL
1 2 3 4 5
CDX2mCherry^pos
b
CDX2mCherry^pos vs. ES
GO:0030198~extracellular matrix organization
GO:0008285~netagive regulation of cell proliferation
GO:0006954~inflammatory response
GO:0045766~positive regulation of angiogenesis
GO:0043066~negative regulation of apoptotic process
GO:0008284~positive regulation of cell proliferation
GO:0007155~cell adhesion
GO:0000122~negative regulation of transcription from RNA polymerase II promoter
GO:0001525~angiogenesis
GO:0045944~positive regulation of transcription from RNA polymerase II promoter
GO:0042493~response to drug
GO:0022617~extracellular matrix disassembly
GO:0007165~signal transduction
GO:0006366~transcription from RNA polymerase II promoter
GO:0006955~immune response
GO:0045892~negative regulation of transcription, DNA-templated
GO:0042060~wound healing
GO:0030335~positive regulation of cell migration
GO:0008584~male gonad development
GO:0070374~positive regulation of ERK1 and ERK2 cascade
GO:0010628~positive regulation of gene expression
GO:0032496~response to lipopolysaccharide
GO:0045893~positive regulation of transcription, DNA-templated
GO:0007267~cell-cell signaling
GO:0006915~apoptotic process
GO:0060021~palate development
GO:0050731~positive regulation of peptidyl-tyrosine phosphorylation
GO:0050727~regulation of inflammatory response
GO:0060337~type I interferon signaling pathway
GO:0048146~postive regulation of fibroblast proliferation
GO:0030324~lung development
GO:0008544~epidermis development
GO:0071407~cellular response to organic cyclic compound
GO:0009612~response to mechanical stimulus
GO:0007565~female pregnancy
GO:0045087~innate immune respvonse
GO:0050918~positive chemotaxis
GO:0001501~skeletal system development
GO:0001558~regulation of cell growth
GO:0030199~colalgen fibril organization
0 5 10 15 20
-log10(Adjusted p value)
e
Vasculature
CDH5
PECAM1
VWF
ACTA2
Log2
10
0
f
Cardiogenesis
HAND2
DKK1
STC2
FHL1
ITGA1
MYOCD
EDN1
TGFB2
Log2
+10
-2
vs. ESC
vs. mCherry^neg
c
AC011228.1
CHCHD2P11
RNU6-1196P
AC018693.2
BX25592.2
AC026401.1
YWHAQP5
AC008868.1
ADORA2A-AS1
AC007950.2
RNF8P0
RAB44
AP003555.2
APOA2
AL050344.1
EPX
CD80
ORM1
HP
PTPRD-AS1
AC003102.1
RUNX3
B3GNT7
RGCC
FGR
SLA
ADAP2
MFSD13A
MAST3
PHACTR1
-12.5
-10.0
-7.5
-5.0
-2.5
-0.0
1 2 3 4
mCherry^neg
1 2 3 4
CDX2mCherry^pos
d
CDX2mCherry^pos vs. CDX2mCherry^neg
GO:0007202~activation of phospholipase C activity
GO:0010873~postive regulation of cholesterol esterification
GO:0019433~triglyceride catabolic process
GO:0042158~lipoprotein biosynthetic process
GO:0007165~signal transduction
GO:0034380~high-density lipoprotein particle assembly
GO:0006909~phagocytosi
GO:0002576~platelet degranulation
GO:0032729~positive regulation of interferon-gamma production
GO:0007155~cell adhesion
GO:0002740~negative regulation of cytokine secretion involved in immune response
GO:0034384~high-density lipoprotein particle clearance
GO:0030593~neutrophil chemotaxis
GO:0001523~retinoid metabolic process
GO:0002309~T cell proliferation involved in immune response
GO:0006952~defense response
GO:0032489~regulation of Cdc42 protein signal transduction
GO:0006935~chemotaxis
GO:0007267~cell-cell signaling
GO:0010903~negative regulation of very-low-density lipoprotein particle remodeling
GO:0034374~low-density lipoprotein particle remodeling
GO:0006954~inflammatory response
GO:0033344~chelesterol efflux
GO:0019886~antigen processing and presentation of exogenous peptide antigen via MHC class II
GO:0050852~T cell receptor signaling pathway
GO:0042157~lipoprotein metabolic process
GO:0006968~cellular defense response
GO:0071346~cellular response to interferon-gamma
GO:0043691~reverse cholesterol transport
GO:0045087~innate immune response
GO:0034375~high-density lipoprotein particle remodeling
GO:0060333~interferon-gamma-mediated signaling pathway
GO:0033700~phospholipid efflux
GO:0050900~leukocyte migration
GO:0007166~cell surface receptor signaling pathway
GO:0002250~adaptive immune response
GO:0042102~positive regulation of T cell proliferation
GO:0050776~regulation of immune response
GO:0031295~T cell costimulation
GO:0006955~immune response
0 5 10 15 20
-log10(Adjusted p value)

Figure 4

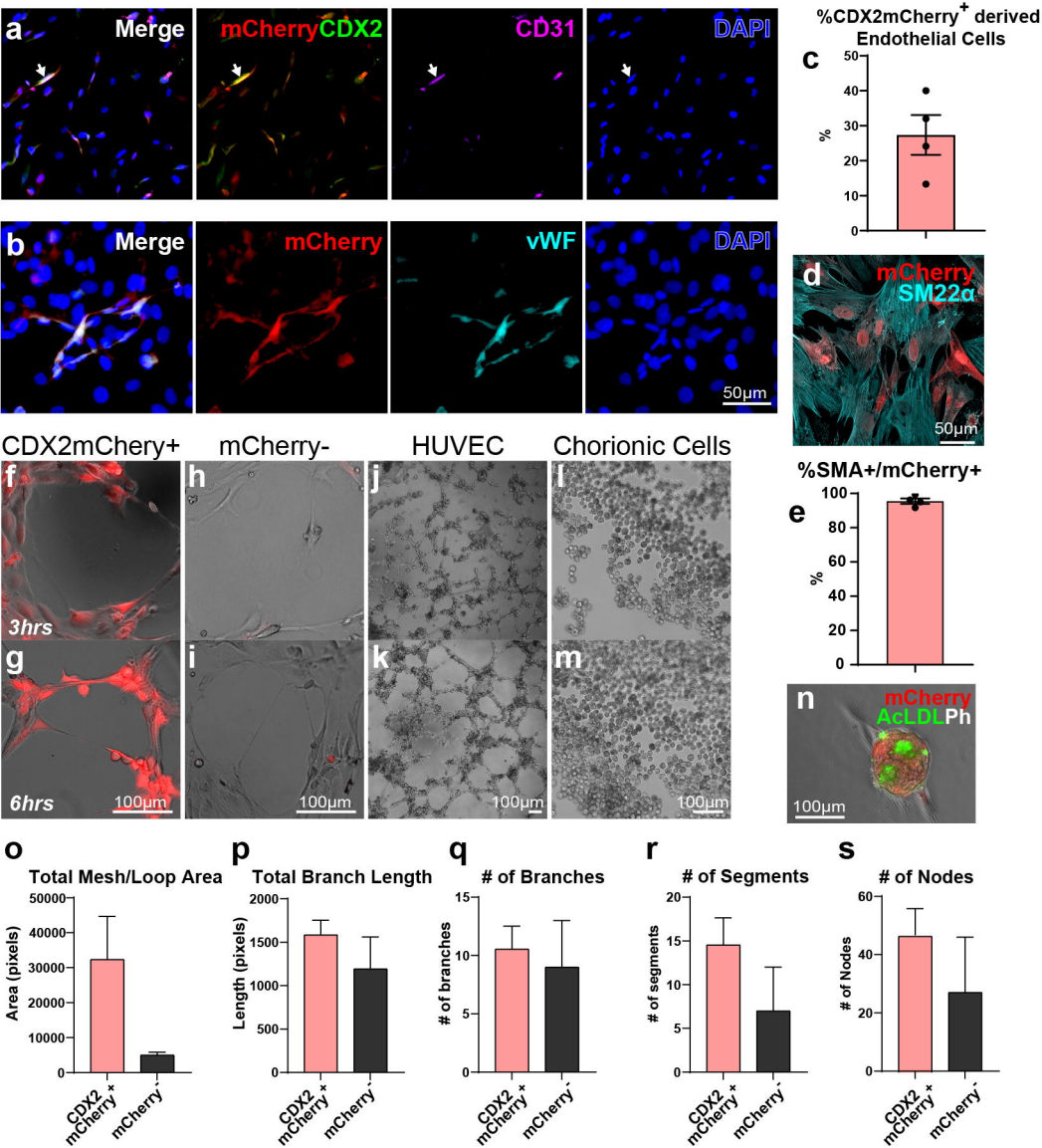
a
Merge
mCherryCDX2
CD31
DAPI
b
Merge
mCherry
vWF
DAPI
50µm
%CDX2mCherry+ derived Endothelial Cells
c
%
d
mCherry
SM22α
50µm
CDX2mCherry+
mCherry-
HUVEC
Chorionic Cells
f
3hrs
g
6hrs
h
i
j
k
l
m
100µm
%SMA+/mCherry+
e
%
n
mCherry
AcLDLPh
100µm
o
Total Mesh/Loop Area
Area (pixels)
p
Total Branch Length
Length (pixels)
q
# of Branches
# of branches
r
# of Segments
# of segments
s
# of Nodes
# of Nodes
CDX2 mCherry+
mCherry-

Figure 5

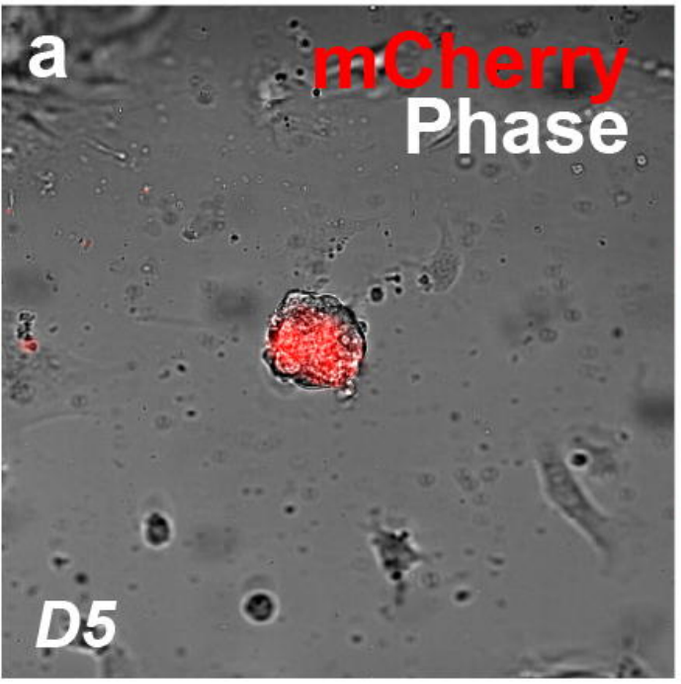
a
mCherry
Phase
D5

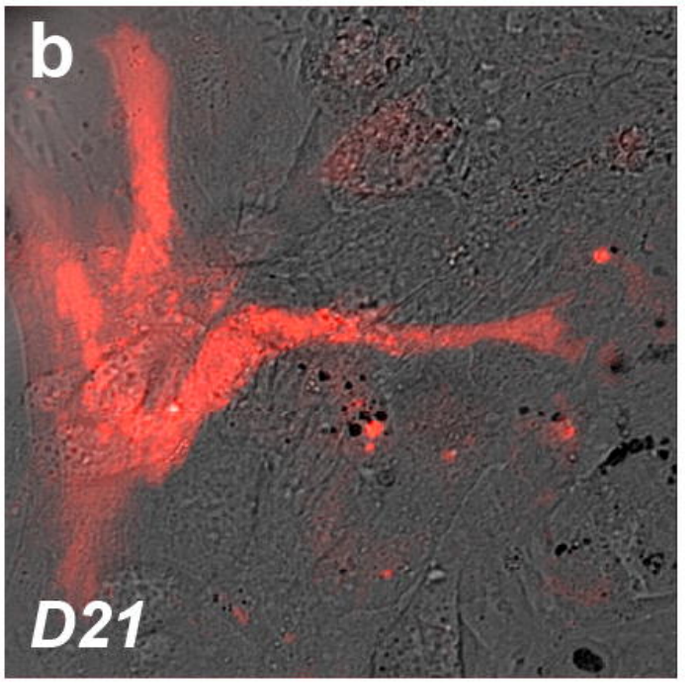
b
D21

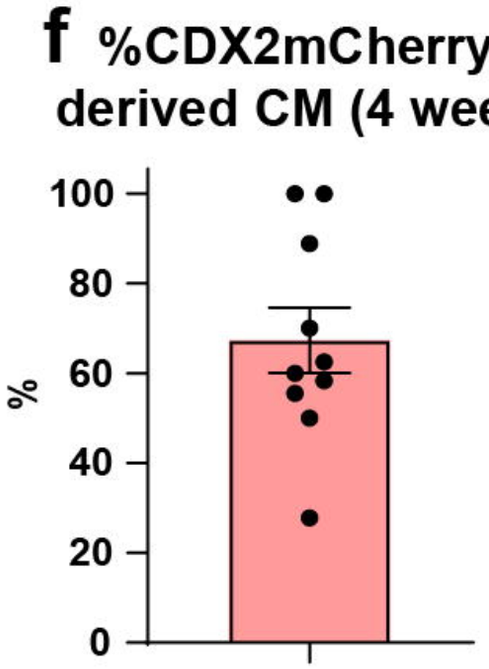
f %CDX2mCherry+ derived CM (4 weeks)
100
80
60
40
20
0
%

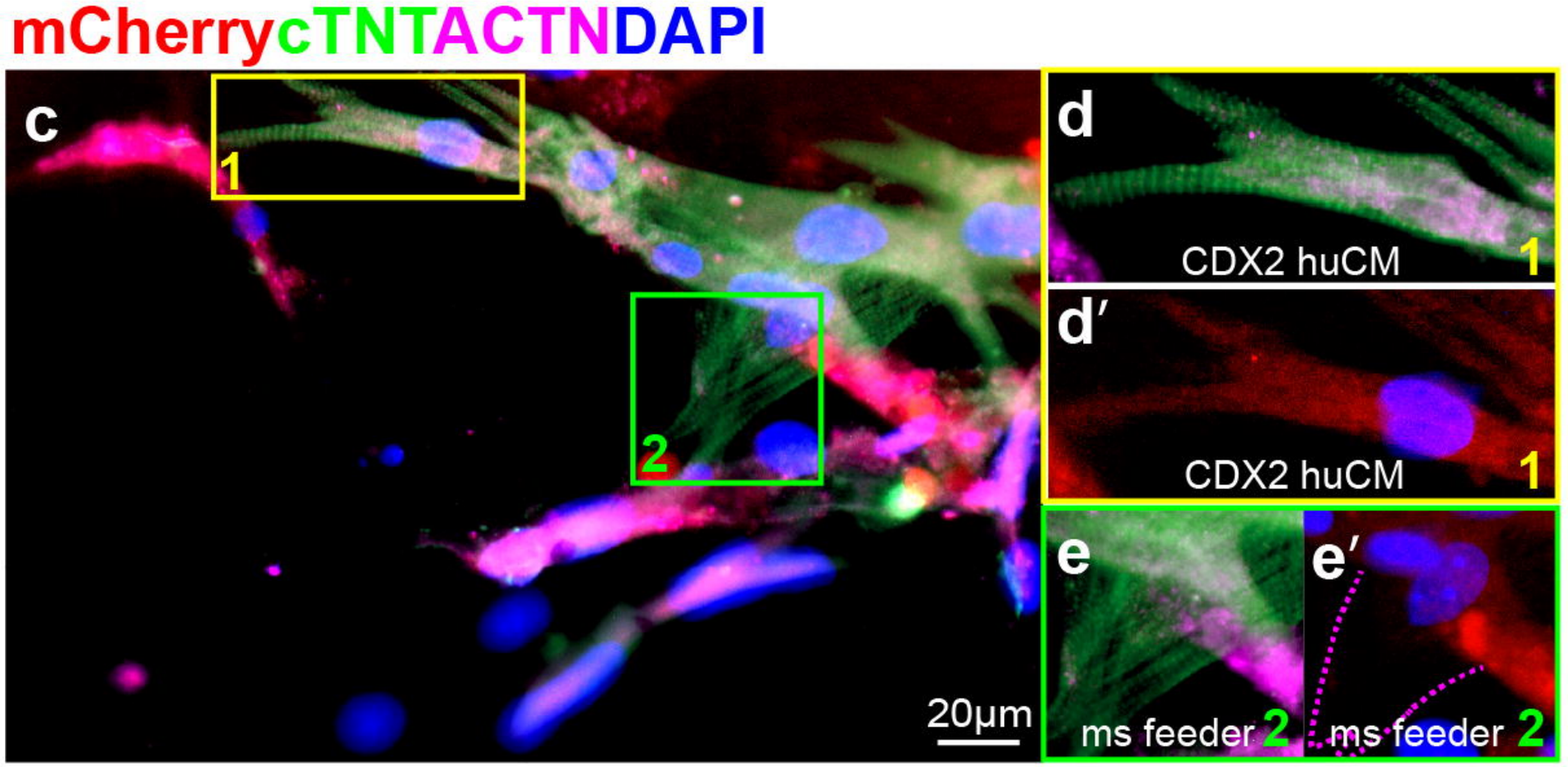
mCherrycTNTACTNDAPI
c
1
2
20µm
d
CDX2 huCM
1
d′
CDX2 huCM
1
e
ms feeder 2
e′
ms feeder 2

Figure S1

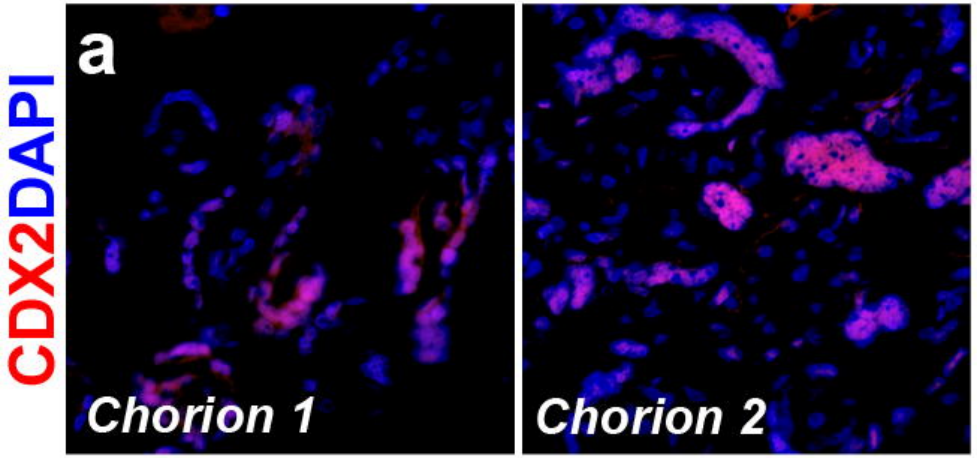
a
CDX2DAPI
Chorion 1
Chorion 2

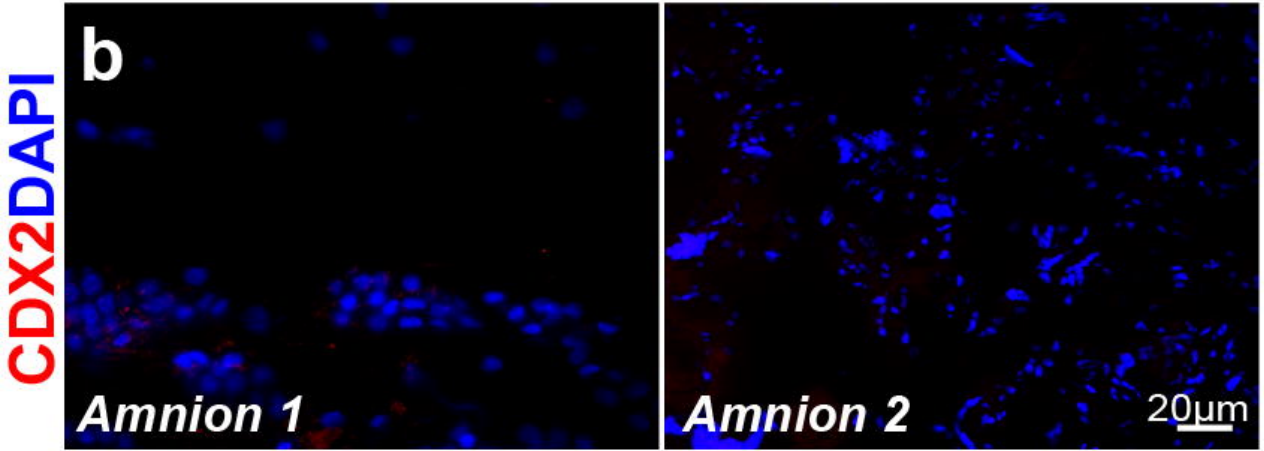
b
CDX2DAPI
Amnion 1
Amnion 2
20μm

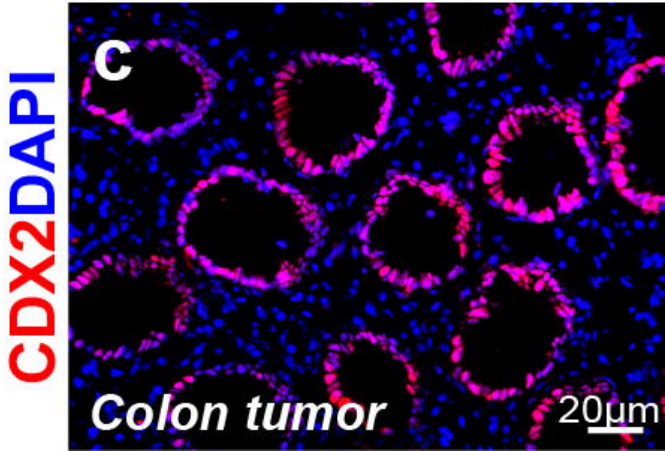
c
CDX2DAPI
Colon tumor
20μm

Figure S2

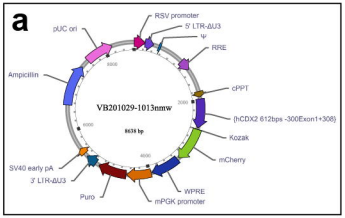

pLV[Exp]-Puro-{hCDX2 612bps -300Exon1+308}>mCherry

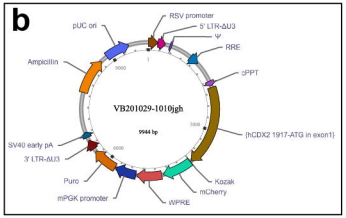

pLV[Exp]-Puro-{hCDX2 1917 -ATG in exon1}>mCherry

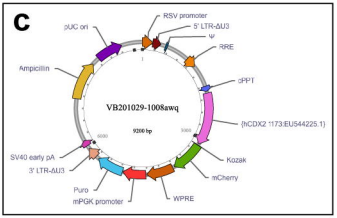

pLV[Exp]-Puro-{hCDX2 1173: EU544225.1}>mCherry

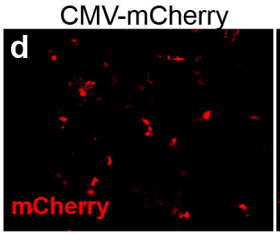

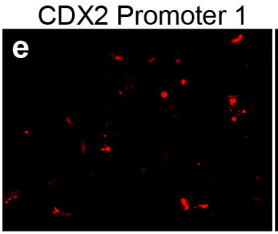

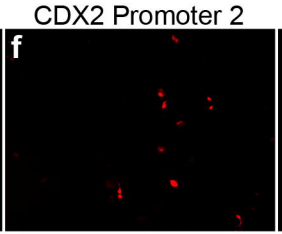

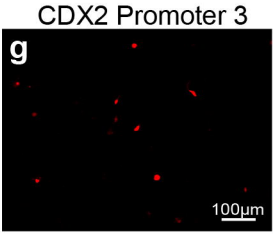

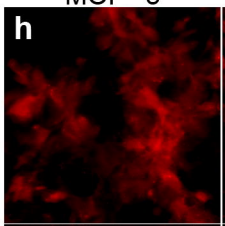

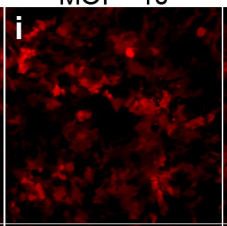

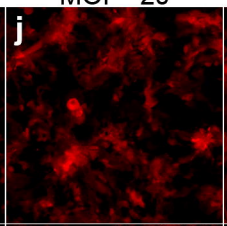

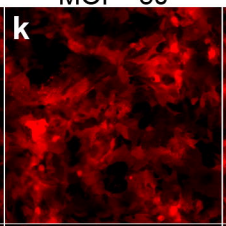

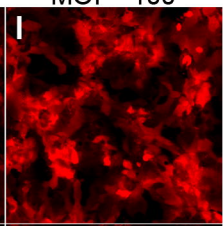

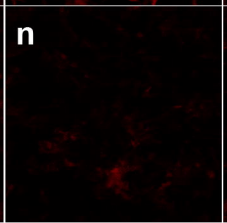

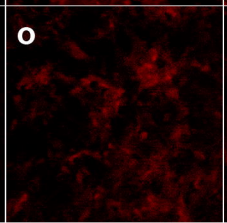

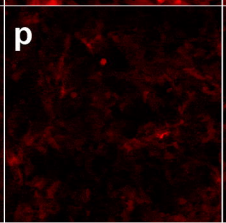

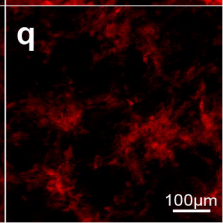

Figure S3

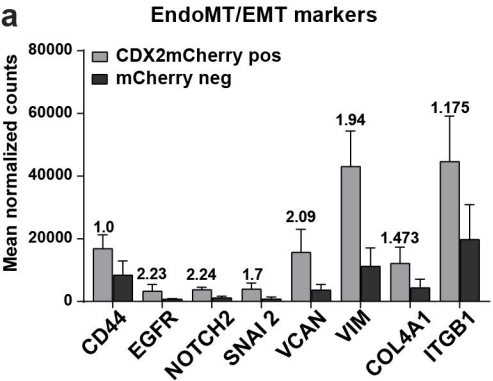
a
EndoMT/EMT markers
CDX2mCherry pos
mCherry neg
Mean normalized counts
80000
60000
40000
20000
0
1.0
2.23
2.24
1.7
2.09
1.94
1.473
1.175
CD44
EGFR
NOTCH2
SNAI 2
VCAN
VIM
COL4A1
ITGB1

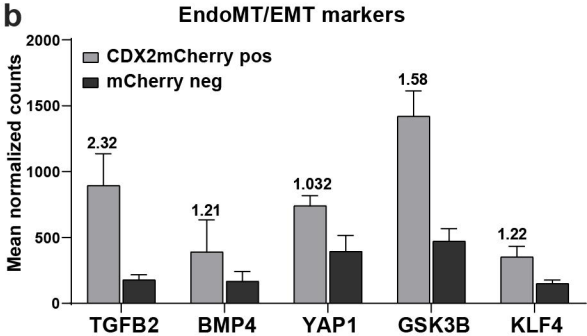
b
EndoMT/EMT markers
CDX2mCherry pos
mCherry neg
Mean normalized counts
2000
1500
1000
500
0
2.32
1.21
1.032
1.58
1.22
TGFB2
BMP4
YAP1
GSK3B
KLF4

Figure S4

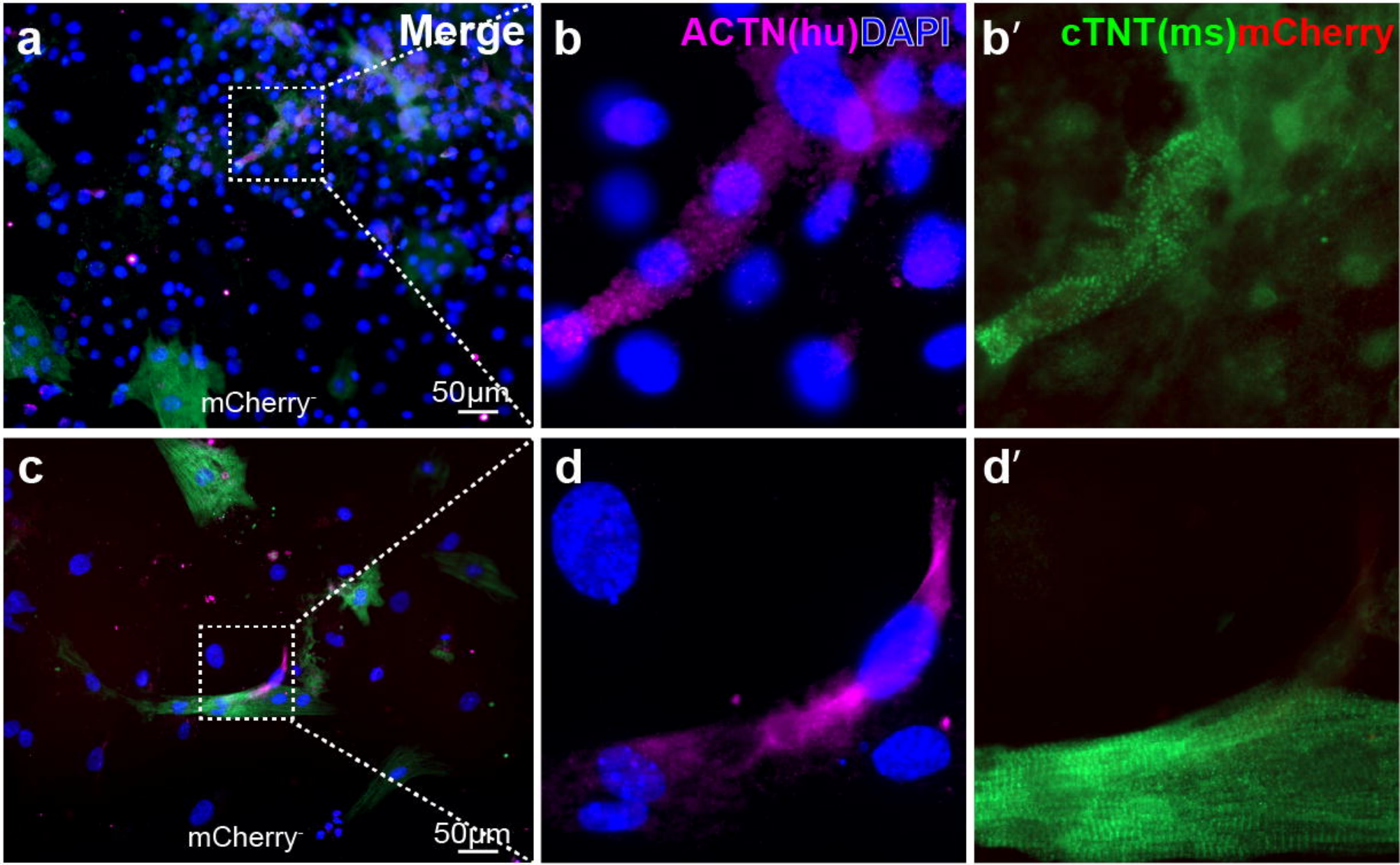
a
Merge
mCherry
50μm
b
ACTN(hu)DAPI
b′
cTNT(ms)mCherry
c
mCherry
50μm
d
d′